RSC Applied Polymers

ROYAL SOCIETY OF CHEMISTRY

PAPER

View Article Online
View Journal | View Issue

Cite this: *RSC Appl. Polym.*, 2026, **4**, 796

Polyhydroxyalkanoate block polymer adhesives derived from long-chain aliphatic β-lactones and lactide

Peter V. Kelly, [a] Alison Block,[b] Brenden D. Hoehn, [a] Pathikrit Saha,[b] Christopher J. Ellison *[a] and Marc A. Hillmyer *[b]

Pressure sensitive adhesives (PSAs) are contained in numerous packaging products as labels, tapes, and sealants. Consequently, they are a common contaminant that complicates repulping during paper recycling and industrial composting. Degradable PSAs are an attractive alternative where complete removal or separation is not practical. In this work, we employed epoxide carbonylation to produce β-tridecalactone to prepare poly(β-tridecalactone) (PTDL) through ring-opening transesterification polymerization (ROTEP). We explored the synthetic challenges in producing high molar mass (>20 kg mol^{-1}) PTDL. These include dehydration of the propagating chain end and adventitious initiation from impurities in the monomer. The utility of PTDL PSAs containing a rubbery midblock with semicrystalline poly(L-lactide) (PLLA) end blocks was probed as a function of composition, molar mass, and processing conditions. The largest PLLA volume fraction (f_{PLLA} = 0.31–0.35) triblock polymers exhibit commercially competitive peel strengths (5.5 ± 0.9 N cm^{-1}) and loop tack (8.5 ± 0.9 N cm^{-1}) values, with properties similar to office and duct tapes. This work informs how long aliphatic chain containing β-lactones can be effectively harnessed to produce high performance PSAs with the end goal of fully biodegradable adhesives.

Received 5th December 2025,
Accepted 6th February 2026

DOI: 10.1039/d5lp00389j

rsc.li/rscapplpolym

Introduction

Pressure-sensitive adhesives (PSAs) are a ubiquitous component of modern commerce. In the low-cost, high-volume market of tapes and films, they can be used to seal packages and affix labels. In higher-cost, lower-volume markets they are used as permanent fasteners in automobiles, provide protective coatings for glass, and support medical devices.[1–3] The prevalence of PSAs found in everyday items leads to the contamination of recycling streams which can cause various problems, particularly in the paper industry where adhesive residues can reduce pulp fiber adhesion and clog processing equipment.[4] PSAs are also found in compost streams and have recently become the target of regulation directed at improving the compostability of produce containing residual adhesive, with the Environmental Protection Agency of Ireland recommending legislation requiring all produce label adhesives be certified compostable.[5] Regulatory trends and the growing awareness of the issues caused by non-degradable plastic waste are leading to efforts to develop degradable PSA formulations.

Polymeric materials that compose PSAs can be broadly grouped into acrylate copolymers,[6] natural rubbers,[7] thermoplastic polyurethanes,[8,9] and styrene block copolymers (SBCs).[10] SBCs are generally ABA triblock polymers composed of glassy poly(styrene) "A" blocks at a minority volume fraction and a rubbery majority "B" block of either poly(butadiene) or poly(isoprene), or hydrogenated analogs. The high glass transition temperature (T_g) hard blocks provide the PSA with the cohesive strength required for high peel forces and shear resistance while the low-T_g rubbery block allows for rapid wetting of substrates on contact.[1] Polyester-based triblock polymers are promising alternatives to SBCs as they can be both biodegradable and sustainably sourced with a wide monomer design space for tailorable properties.[11,12] A growing body of work has explored PSA formulations with poly(lactide) (PLA) hard blocks and a variety of lactone-based midblocks such as poly(menthide),[13] poly(β-methyl-δ-valerolactone),[14] poly(pentadecyl caprolactone) (PPDCL),[15] poly(γ-methyl-ε-caprolactone) (PγMCL),[16] poly(*n*-alkyl-*δ*-lactone),[17] and poly(ε-decalactone)[18] synthesized by ring-opening transesterification polymerization (ROTEP). Many of these low-T_g polyester based midblocks have low entanglement molar masses (M_e) which decrease their

[a]*Department of Chemical Engineering and Materials Science, University of Minnesota, Minneapolis, Minnesota 55455, USA. E-mail: cellison@umn.edu, hillmyer@umn.edu*
[b]*Department of Chemistry, University of Minnesota, Minneapolis, Minnesota 55455, USA*

ability to bond to a substrate and thus require the addition of tackifier in PSA formulations.[15]

Long-alkyl chain β-lactones are a promising class of monomers that could be viable midblocks for biodegradable triblock PSAs. β-lactones can be produced from plant oils, using long-chain alpha olefins which are a product of olefin metathesis as a starting material, followed by epoxidation and carbonylation.[19,20] The length of the aliphatic side chain can be tuned to increase the corresponding polymer M_e. For example, Kim *et al.* demonstrated that the 15-carbon pendent group on PPDCL resulted in an M_e of 20–28 kg mol^{-1} and Schneiderman *et al.* showed that increasing the chain length of substituted *n*-alkyl-δ-lactone from a methyl to pentyl raised M_e from 3.4 to 13.5 kg mol^{-1}.[15,21] MacDonald *et al.* has explored the polymerization of β-lactones with methyl, ethyl, *n*-butyl and decyl pendent groups and demonstrated that the shorter pendent group monomers can successfully produce ABA triblock polymers with PLLA end blocks *via* ROTEP. However, they did not pursue the decyl substituted monomer due to slow polymerization kinetics.[22]

In this work we demonstrate, for the first time, the use of long-chain 1,2-epoxides as the starting material for the synthesis of β-lactone based polyester triblock PSAs. Derivable from bio-based long-chain fatty acids, 1,2-epoxides provide a diverse class of materials from which to design high entanglement molar mass midblocks. We demonstrate that this synthetic approach is viable by synthesizing β-tridecalactone (TDL) *via* epoxide carbonylation of 1,2-epoxydodecane (EDD) and, through subsequent ROTEP steps, produce ABA triblock polymers with hard, semicrystalline PLLA end blocks and soft poly(β-tridecalactone) (PTDL) midblocks. We discuss the synthetic challenges surrounding the polymerization of β-lactones and develop PSA formulations which are competitive with commercial materials, demonstrating that long-chain β-lactones are promising candidates for future development of more sustainable PSAs from agricultural feedstocks.

Results and discussion

Monomer synthesis and polymerization

The synthesis of TDL and the subsequent polymerization details are included in the SI. Epoxide carbonylation is a well-established method to produce β-lactones with good selectivity, preservation of stereocenters, and high yields when optimized.[23,24] Coupled with the industrialization of long-chain epoxidized alpha-olefins, such as Cargill's Vikoflex®, this chemistry introduces opportunities in materials development using long-chain β-lactones to produce PSAs (Scheme 1a). The primary side product of this carbonylation is a ketone produced *via* β-elimination of the ring-opened epoxide which is favorable at low CO pressures and high temperatures.[25,26] Synthesis of TDL was conducted at 560 psig of CO and 60 °C with the ratio of epoxide to catalyst tuned to reduce the production of the corresponding ketone (dodecan-2-one), with a selectivity of 97% achieved by reducing catalyst loading to 0.04 mol% of the epoxide (Table S1). The characterization of the products by ^{1}H and ^{13}C NMR spectroscopy (Fig. S1–4) is included in the SI. Catalyst removal and vacuum distillation of the monomer was carried out before a single-pot triblock synthesis of LTL was performed, as shown in Scheme 1b.

Several challenges exist in synthesizing high molar mass hydroxy-telechelic polyhydroxyalkanoates *via* ring-opening polymerization of β-lactones. The two most relevant to this work being the competition between *O*-acyl and *O*-alkyl bond cleavage (nucleophilic attack at the carbonyl carbon or the tertiary carbon in the ring) producing either a carboxylate-containing chain end or a hydroxyl-containing chain end, respectively, and the dehydration of the propagating secondary alcohol from *O*-acyl cleavage leading to chains with unsaturated end groups.[27] These side-reaction products are detrimental to the synthesis of block polymers as both carboxylic acid and dehydrated end group types are unable to initiate subsequent block polymerization *via* ROTEP. We tested commonly used catalysts from literature including trifluoromethanesulfonic acid (HOTF), bis(4-nitrophenyl) phosphate (BNPP), diphenyl phosphate (DPP), and triethyl aluminum (Et_3Al) with the goal of achieving molar masses above 20 kg mol^{-1} and low degrees of dehydration. The Lewis acid, Et_3Al, was chosen for its ability to produce high end-group fidelity. In our polymerization, BDM initiated ROTEP of TDL catalyzed by Et_3Al was employed to produce hydroxy-telechelic PTDL macroinitiators. After polymerization of TDL to ~90% conversion (^{1}H-NMR spectroscopy), L-lactide was added to produce the corresponding LTL triblock polymers. ^{1}H NMR spectroscopy (Fig. 1) indicated that the desired terminal methine from poly(β-tridecalactone) appeared as a broad peak (δ 3.9 ppm), while the presence of the dehydrated end groups formed during TDL polymerization presented as a doublet (δ 5.75 ppm) and multiplet (δ 6.9 ppm).[28] After the addition of L-lactide, the integrations of the olefinic end groups remained the same suggesting no further increase in their concentration and that they did not participate in chain extension with L-lactide (Fig. 1). Complete initiation from the PTDL hydroxyl groups was observed in the second step, with the appearance of PLLA terminal methine protons (δ 4.3 ppm) and the disappearance of the PTDL terminal methine protons (δ 3.9 ppm). A consequence of some chain-end dehydration is that three species are present in the final block polymer sample: the desired LTL triblock polymers, PTDL-*block*-PLLA diblock polymers corresponding to one dehydration event on one end of the growing telechelic PTDL macroinitiator, and PTDL homopolymer with two dehydrated chain ends, as shown in Scheme 1b.

Four LTL samples were synthesized with $M_{n,PTDL}$ targets of 19 and 38 kg mol^{-1} and f_{PLLA} targets of 0.125 and 0.25. The labeling of the materials is LTL ($M_{n,PTDL}$, f_{PLLA}) with the molecular characteristics listed in Table 1 and the synthetic conditions in Table S2. Size exclusion chromatographic (SEC) analysis of the PTDL macroinitiators and chain-extended polymers corroborate the ^{1}H NMR spectroscopic evidence of block polymer formation (Fig. S5), with clear shifts in the peak elution times. The traces in Fig. 2 provide qualitative evidence

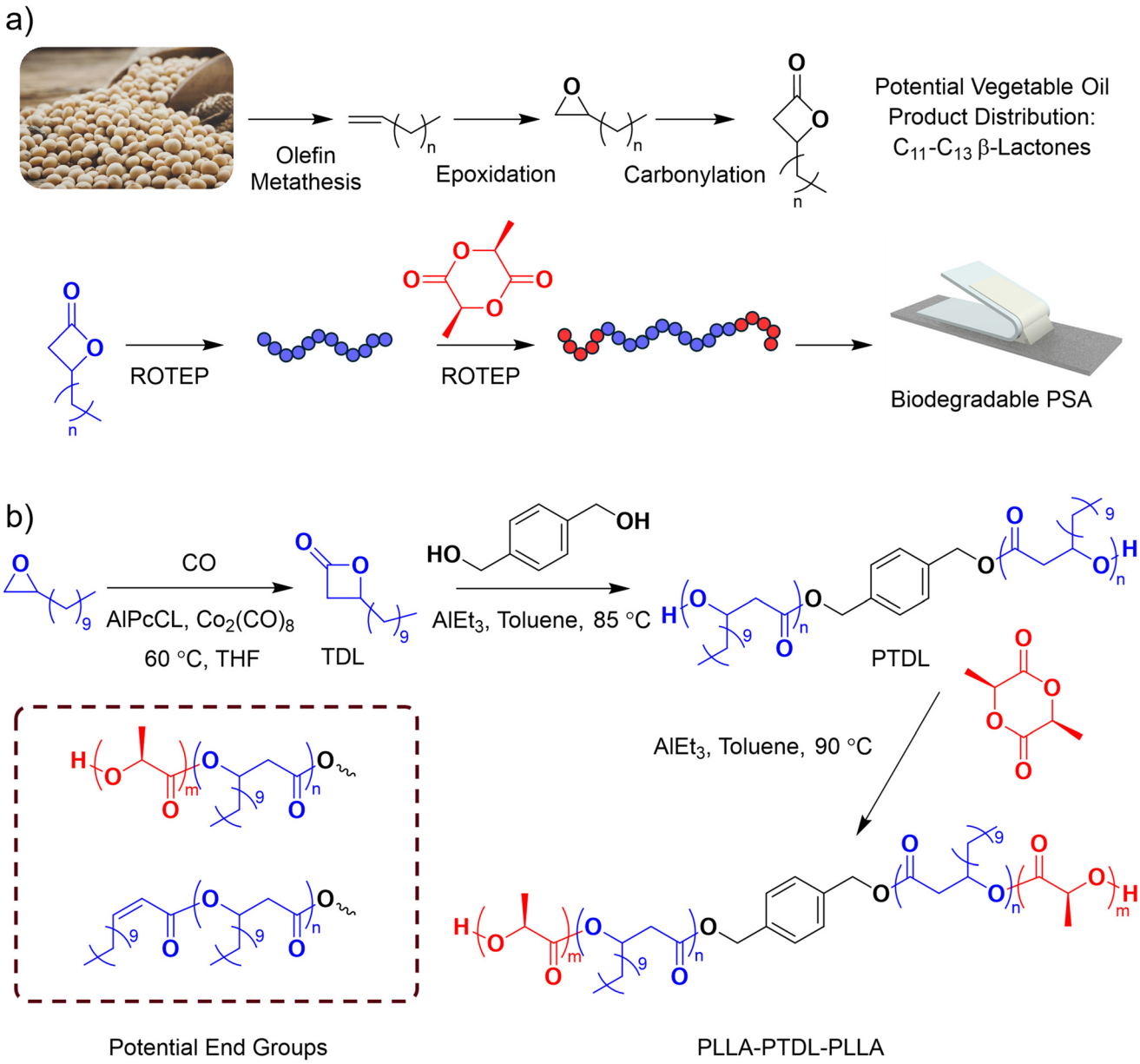

Scheme 1 (a) Representative pathway from vegetable oils to biodegradable PSAs *via* long-chain β-lactones produced through the epoxidation of alpha-olefins and carbonylation of subsequent 1,2-epoxides followed by ROTEP and chain extension with PLLA. (b) Synthetic scheme for the synthesis of PLLA-PTDL-PLLA triblock polymers. Carbonylation of 1,2-epoxydodecane to produce β-tridecalactone is followed by ring-opening polymerization initiated by 1,4-benzene dimethanol to produce telechelic poly(β-tridecalactone). Subsequent chain extension with L-lactide produced LTL triblock polymers. In addition to the primary triblock polymer product, the end groups of possible dehydrated side products are shown in a dashed box.

for the presence of LTL triblock, TL diblock, and PTDL homopolymer, with the LTL sample traces appearing trimodal. A broader distribution is already apparent in the higher molar mass PTDL macroinitiators before chain extension, with a high molar mass shoulder appearing. Increasing dispersity is noted in Table S2 after chain extension to produce PLLA endblocks, likely the result of doubly-dehydrated PTDL chains not extending and PLLA-PTDL diblock polymers forming with lower total molar mass than the final triblock polymers, broadening the overall distribution of chain lengths. The ^{1}H NMR spectroscopic analyses (details in the SI, Fig. S6, and Table S3) show a larger percentage of dehydrated chain ends in the higher M_n triblock polymers, with the ratio of dehydrated end groups to initiator species increasing from approximately 25% in the systems with ~16 kg mol^{-1} PTDL based macroinitiators to approximately 50% in the ~34 kg mol^{-1} PTDL macroinitiator based triblock polymers. This could be the result of the longer reaction time (40 h *vs.* 80 h, respectively) providing more

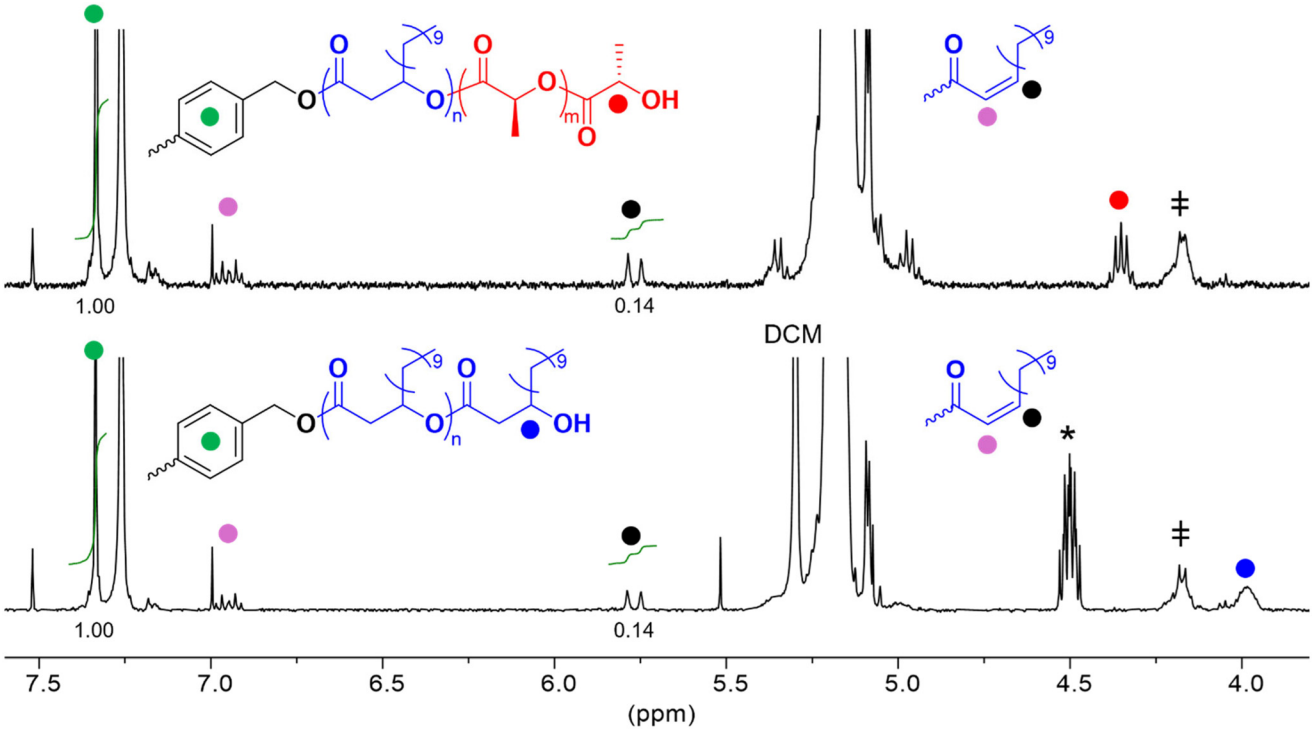

Fig. 1 ^{1}H NMR (400 MHz, $CDCl_3$) spectra of the 17 kg mol^{-1} PTDL homopolymer (bottom) and LTL (17k, 0.35) (top) highlighting the disappearance of the terminal methine signal of the PTDL (blue) upon chain extension with PLLA (new end groups shown in red). The alkene protons of the dehydrated end group are unreactive to chain extension and do not change in intensity during this process (black). Integrations of the aromatic protons on the BDM initiator and the doublet from the dehydrated end group are shown under the spectra for reference. *Residual monomer. ‡Tentatively assigned to methylene protons from an ethyl ester impurity.

Table 1 Molar mass and end-group analysis of LTL triblock polymers

Sample	$M_{n,PTDL}$[a] (kg mol^{-1})	f_{PLLA}[b]	$M_{n,PLLA}$[c] (kg mol^{-1})	$Đ$[d]	End-group fidelity[e]
LTL (16k, 0.18)	16.3	0.18	3.6	1.2	72%
LTL (17k, 0.35)	16.5	0.35	9.7	1.4	76%
LTL (34k, 0.21)	34.1	0.21	5.8	1.3	49%
LTL (35k, 0.31)	35.4	0.31	9.8	1.3	49%

[a] Calculated from the relative integrations of PTDL repeat units and BDM aromatic protons from ^{1}H NMR spectroscopy. [b] Calculated from PTDL and PLLA repeat unit integrations from ^{1}H NMR spectroscopy. [c] Calculated from the PLLA repeat units and terminal methine end groups. [d] Dispersity calculated from RI SEC trace with polystyrene standards. [e] Ratio of non-dehydrated end groups to BDM initiator sites as determined by ^{1}H NMR spectroscopy integration.

opportunities for dehydration after higher monomer conversions. An increase in the ratio of total end groups to initiator species is also noted in these higher molar mass LTL samples with both LTL (35k, 0.31) and LTL (34k, 0.21) having approximately one dehydrated end group and two PLLA end groups per BDM initiator. This is likely due to the adventitious initiation of PTDL by the water released from dehydration of propagating end groups, as the $AlEt_3/H_2O$ system is a known initiator of β-butyrolactone and likely TDL.[29,30] Consequently, the true molar masses of the PTDL midblock are likely lower than those calculated in Table 1. The SEC data in Table S2 shows that the higher molar mass targets (PTDL (34k) and (35k), respectively) and the lower molar mass targets (PTDL (16k) and (17k), respectively) may have more similar molar masses than the ^{1}H NMR data would suggest. The presence of diblock polymers in a triblock-based PSA formulation has been shown to affect the mechanical properties of fibrillation during tack experiments but their inclusion in a formulation does not compromise the materials applicability as an adhesive.[31,32]

PSA microstructure and thermal properties

Neat LTL solutions were made by dissolving the LTL samples in chloroform with a final solids content of 20 wt%. Solutions were blade coated onto a semicrystalline PET backing with a 1 mm gap and allowed to dry under an active nitrogen flow for 48 h and gave final film thicknesses of approximately 110 μm. No residual solvent was observed in the films by differential scanning calorimetry (DSC) analysis after drying. The mechanical utility of a triblock-based PSA is predicated upon the microphase separation of the hard and soft domains,[33] where the hard domains provide cohesive strength to the film and the soft domain allows for wetting of the substrate under light pressure. Previous work using solvent casting for PSA preparation found the resultant block polymer microstructure is heavily dependent on processing conditions, and that kinetically trapping a disordered state can occur even when long-

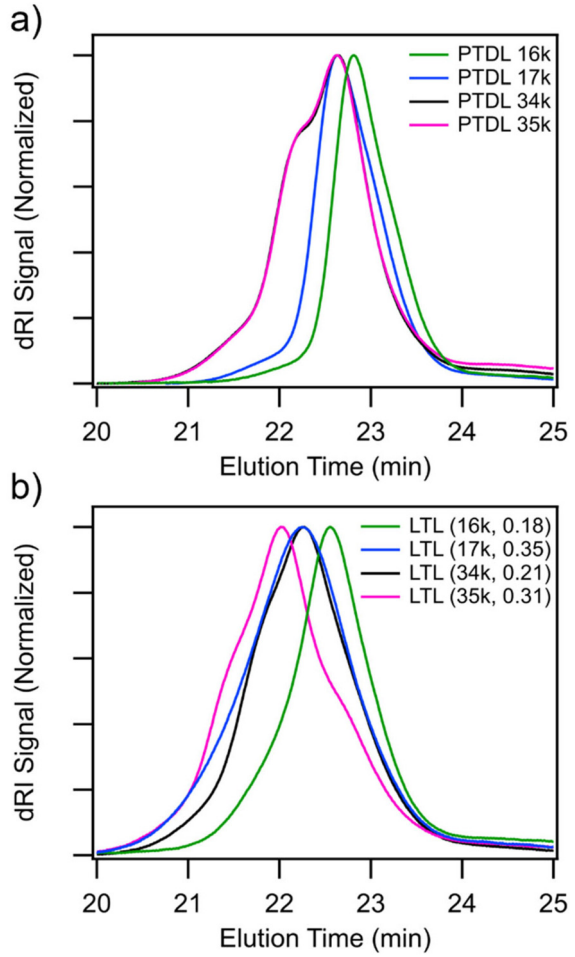

Fig. 2 (a) SEC elution traces of PTDL macroinitiators isolated from the one-pot synthesis of LTL triblock polymers. (b) SEC elution traces of LTL triblock polymers after synthesis and purification showing block formation and a multi-modal distribution.

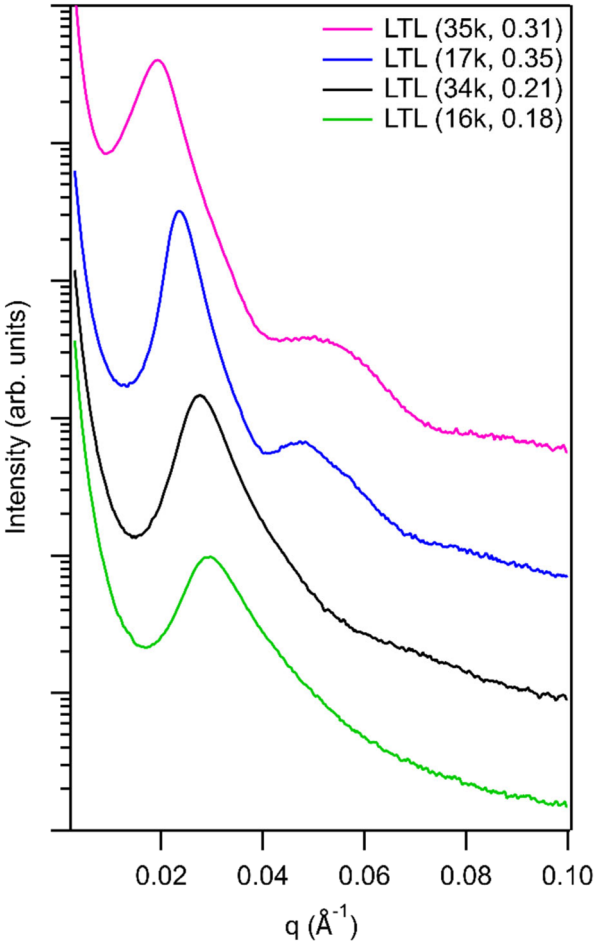

Fig. 3 SAXS patterns of neat LTL triblock PSA samples after solvent casting from chloroform and drying under nitrogen demonstrating microphase separation. Data vertically shifted for clarity. Samples have the same processing history as adhesion samples and DSC samples.

range order is possible in the system.[34] As an example, using a similar solvent casting method as in this work, Liang *et al.* demonstrated that for PγMCL-based triblock PSAs solvent casting resulted in poorly ordered microstructures; high-temperature annealing produced strongly segregated domains and desirable adhesive properties.[16] Small angle X-ray scattering (SAXS) of our neat, as-cast LTL triblock films reveal intense principle scattering peaks (q^*), indicative of microphase separation, with domain spacings ranging from 21 to 34 nm (Fig. 3 and Table S4). Microphase separation of the blocks was further supported by the presence of independent T_gs for each block in the DSC traces (Fig. S8). The more pronounced microphase separation of the LTLs after solvent casting in this system could be the result of the relatively low molar mass of these polymers or the presence of diblock polymers as described above.[35]

In the high PLLA volume fraction triblock materials, LTL (35k, 0.31) and LTL (17k, 0.35), broad form factor scattering in the SAXS data is observed, which could indicate spherical or cylindrical domains. The lack of distinct higher-order peaks prohibits a definitive identification of the microstructure, with the samples best described as locally microphase separated but poorly ordered over longer length scales. This behavior has been observed in similar systems with PγMCL midblocks and PLLA end blocks and is often attributed to kinetic trapping of the block polymer microdomains during processing.[36–38] Fitting to cylindrical and spherical form factors were attempted for both samples and show large deviations between the fitted radii and the radii calculated using the principle scattering peak (Table S5), indicating that neither form factor well describes this system. The lower volume fraction samples exhibited only principle scattering peaks which indicate that they are locally microphase separated without long range order. These poorly defined domains are expected to decrease the adhesive performance of the PSA formulations.[16]

Microphase separation and well-ordered domains are important for block polymer adhesives, but they are not sufficient for good adhesive performance. The midblock must also be rubbery at the use temperature and exhibit facile substrate adhesion. This often requires incorporation of small

molecule tackifiers to reduce the elastic moduli of the materials. The addition of tackifier to triblock based PSA formulations dilutes the entanglements of the midblock, allows effective wetting of the substrate, and has been shown to improve adhesion in the case of high M_e midblocks, such as PPDCL.[14,15]

We prepared PSA formulations of the four LTL triblocks at different tackifier loadings (ranging from 0–60 wt% tackifier) using the rosin ester tackifier, Sylvalite RE 80HP, to understand how tackifier content affected the adhesive properties of the PSAs. It is important for the tackifier to segregate preferentially into the rubbery midblock domains and not compromise the cohesive strength afforded by the hard endblock domains. To probe the miscibility of tackifier into our block polymers, we analyzed the thermal properties and microstructure of these blends. Changes in the T_gs, as determined by the DSC data shown in Fig. 4, of the two blocks as a function of tackifier loading can be used to understand its partitioning into the respective domains. An increase in the PTDL T_g from −42 °C to −18 °C was observed between 20 and 60 wt% tackifier loading, whereas a negligible decrease in PLLA T_g was observed. This trend was consistent across all LTL samples in both the first (only PLLA T_g observable) and second heating cycles (Table S4 and Fig. S7–9) and supports the tackifier preferentially segregating into the PTDL phase. Similarly, SAXS analysis of the PSA formulations with tackifier shows that the form factor scattering behavior is not significantly affected by its addition (Fig. S10), with the broad single peaks of these samples indicating a poorly ordered but microphase separated morphology (as evidenced by the distinct glass transition temperatures seen in the DSC traces in all triblock polymer samples with tackifier). We also noted a lack of PLLA crystallinity in the first DSC heating traces (Fig. S7) and verified this by WAXS analysis (Fig. S11). This is likely due to the rapid evaporation of solvent during casting, preventing crystallization of the PLLA end blocks. End block crystallinity has been shown to increase PSA performance and could be achieved by an annealing step above the T_g and below T_m of PLLA.[16] The lack of PLLA melting in the second-heating cycle (Fig. 4) is explained by the slow crystallization of PLLA, with no crystallization exotherm observed in the cooling traces (Fig. S9).

A striking feature in Fig. 4 is the melting endotherm at −26 °C in the 0 wt% tackifier sample. The same behavior is observed in all neat LTL samples (Table S2 and Fig. S8) with the corresponding crystallization exotherm in the relevant cooling traces (Fig. S9). We attribute this to the crystallization of the aliphatic side chain attached to the PTDL backbone. Similar side-chain crystallization was also observed by Kim *et al.* in their study of PPDCL, with the 15-carbon side chain melting at 27 °C and the percent crystallinity of the midblock decreasing as a function of tackifier loading.[15] The authors made the comparison to the melting of poly(*n*-alkyl acrylates) which show an increasing melting temperature (T_m) as a function of side-chain length, with a side-chain length greater than 9 carbons required for crystallization to occur.[39] Interestingly, in our PSA formulations, tackifier completely suppresses the side-chain crystallization above a 20 wt% loading.

Further analysis of the T_g of the PTDL homopolymer using the Fox equation and the measured T_gs of the PTDL in the PSA samples with different tackifier loadings is instructive. From this analysis (details in the SI) we estimate that the T_g of the PTDL homopolymer is approximately −50 °C but obscured in the DSC data due to side chain crystallization. Crystallization of a PSA's midblock can limit its useful temperature range, as below this T_m the midblock cannot easily flow and form a bond with the substrate. In the case of PTDL, the low side-chain melting point and suppression of crystallization when formulated with tackifier permit usage of the material at a wide range of temperatures.

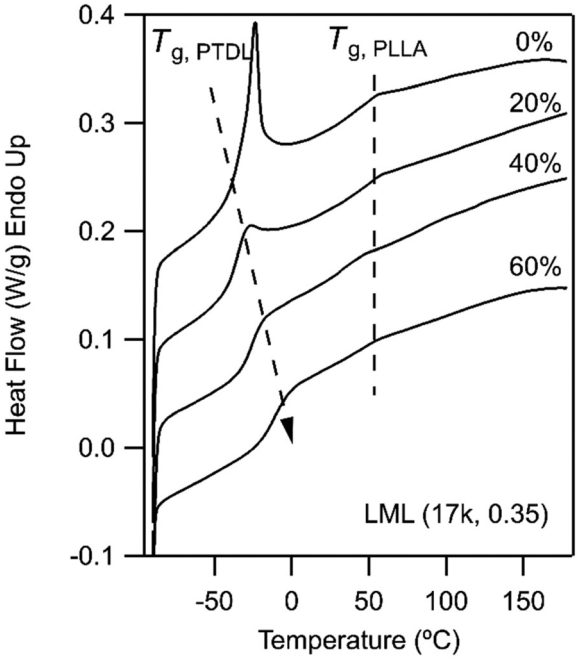

Fig. 4 DSC traces of LTL (17k, 0.35) PSA formulations showing the glass-transitions of the PTDL midblock and PLLA end blocks at different wt% tackifier loadings, indicated by the percentages on the right. At 0 wt% tackifier loading a melting endotherm overlaps with the T_g of PTDL. Traces vertically shifted for clarity, second heat (10 °C min^{-1}) shown. Samples have the same processing history as adhesion test samples and SAXS samples. Measurement details included in the SI.

PSA rheology

To understand the potential application space for these materials rheological analyses were conducted. The materials were loaded into the rheometer at elevated temperatures and then cooled making their thermal history more like the second DSC heating traces than the as-tested adhesives. PSA formulations are often heated during industrial processing and as such these measurements provide insights into their potential behavior. Time–temperature superposition (TTS) was employed to construct master curves of the storage (G') and loss (G'') moduli of PSAs at 0 and 40 wt% tackifier loadings. In Fig. 5a the master-curves for LTL (35k, 0.31) show the onset of the rubbery-plateau region at lower frequencies along with the

glass transition of the PTDL midblock in the 40 wt% tackifier sample at the higher-frequency range of the curve. In the 0 wt% tackifier formulation, crystallization of the aliphatic side chains in the PTDL caused the TTS to fail below −20 °C and so the glass transition for that sample is not resolvable. Similarly, at 60 °C and higher the glass transition of the PLLA end blocks caused the TTS to fail and as such the data is best interpreted between those values. All formulations satisfy the Dalquist criteria (Fig. S12), which stipulates that for fast adhesion of a PSA to a substrate the G' should fall below 0.3 MPa at room temperature and a frequency of 1 rad s^{-1}. The addition of tackifier further lowers this G' with the LTL (35k, 0.31) sample falling from 0.10 MPa to 0.05 MPa with the addition of 40 wt% tackifier as expected. Master-curve data can be used to analyze the application space of PSAs *via* Chang's window analysis.[40] A PSA's position in the four quadrants helps to identify its appropriate use conditions. Fig. 5b shows the corresponding analysis for the high f_{PLLA} triblock polymers at 0 and 40 wt% tackifier loading. Their position in the upper-right quadrant indicates that they would be high-shear resistant PSAs. The large values of G' and G'' in the top-right corner of the window predict high peel forces upon removal while the G' at the bottom two points of the window predict good shear performance due to the elastic characteristic of the samples.

Adhesive performance

The peel and loop tack testing data (Fig. 6, Table S6, and Fig. S13–20) shows how the synthesized LTL triblock polymers performed once formulated with tackifier and solvent cast onto the PET backing. All neat LTL triblock polymers, except for LTL (34k, 0.21), demonstrated negligible average peel forces. We believe that the high PLLA volume fractions of these materials make them behave more elastically without tackifier and thus they easily debond and experience adhesive failure. This elastic behavior is corroborated by rheological testing, in which the tackifier-free sample demonstrated solid-like behavior at all tested frequencies (Fig. 5a and Fig. S12). With the addition of tackifier, differences become apparent between the low and high PLLA volume fraction triblock polymers. The lower PLLA volume fraction triblock PSAs failed cohesively at 20 wt% tackifier and above, as shown by the residual PSA in Fig. S21 after testing. This trend was also seen in the loop tack data in Fig. 6b. We hypothesize that this is due to a combination of the poor microphase separation of the materials noted in the SAXS data and the low molar mass of the PLLA end blocks leading to more facile chain pullout from the hard domains.[41] In contrast, the larger volume fraction triblock polymers, LTL (17k, 0.35) and LTL (35k, 0.31), demonstrate adhesive failure from the substrate (Fig. S22), with higher peel strength (2.1 ± 0.3 N cm^{-1} and 5.5 ± 0.9 N cm^{-1} respectively) and loop tack (3.8 ± 0.2 N cm^{-1} and 8.5 ± 0.9 N cm^{-1} respectively) values achieved with increasing tackifier loading up until 60 wt% tackifier, at which point a stick-slip behavior is observed and testing had to be conducted at lower peel rates (Fig. S13–S20). We hypothesize that this switch in failure mode is due to more complete microphase separation of the PLLA

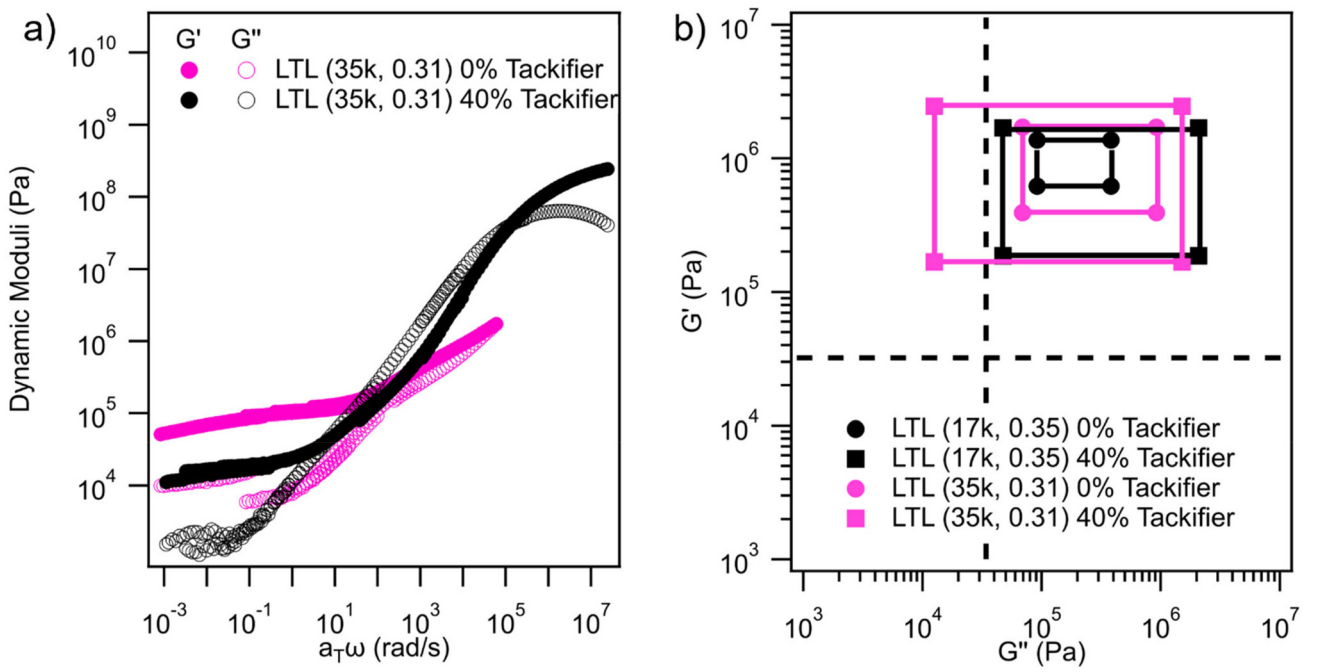

Fig. 5 (a) Storage (closed circles) and loss (open circles) moduli master curves of LTL (35k, 0.31) triblock-based PSA formulations at two tackifier loadings, 0 wt% (pink) and 40 wt% (black). The reference temperature used to determine the shift factors was 20 °C. (b) Chang's window analysis showing the viscoelastic behavior of selected LTL (35k, 0.31) and LTL (17k, 0.35) PSA formulations at 100 rad s^{-1} and 0.01 rad s^{-1} from master curves constructed with a reference temperature of 20 °C. Dashed lines separate the window into quadrants delineating appropriate applications based upon PSA behavior during bonding and debonding.

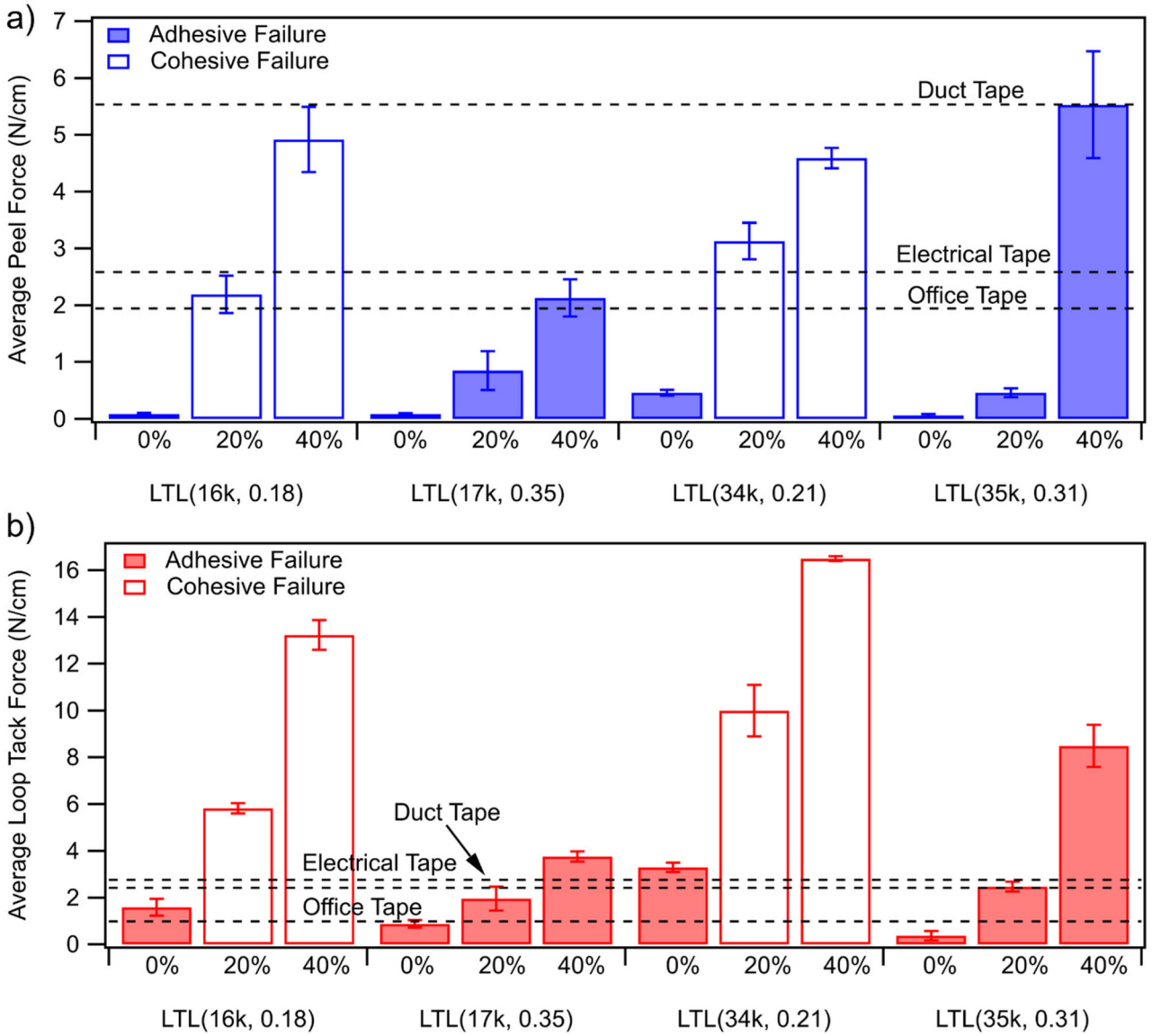

Fig. 6 (a) Average peel force measurements of solvent-cast LTL triblock PSAs with the weight fraction of tackifier listed below each bar. (b) Average loop tack force measurements of solvent cast LTL triblock PSAs. Solid bars represent adhesive failure between substrate and PSA while open bars represent cohesive failure of the PSA. Error bars represent one standard deviation above and below the average. 60 wt% tackifier values not plotted as they required a lower displacement rate to avoid stick-slip behavior. Commercial product properties from reference Kim *et al.*[15]

hard domains, consistent with the appearance of higher order features in the SAXS patterns. A better developed microstructure provides more mechanically effective hard domains and increases the cohesive strength of a PSA film.[16] The superior performance of the LTL (35k, 0.31) triblock sample at 40 wt% tackifier, achieving an average peel force of 5.5 ± 0.9 N cm^{-1} and a loop tack value of 8.49 ± 0.9 N cm^{-1}, makes this material comparable to high-strength commercial PSAs such as duct tape.

The shear resistance of the formulations was analyzed by suspending a 0.25 kg weight from a 1.27 cm x 1.27 cm square of PSA for 10 days (Fig. S23). Shear resistance testing (Table S6) shows that at tackifier loadings of 20 wt% and lower, the high-volume fraction triblock PSAs exhibit excellent longevity, with no failure of three replicates over a 10-day period. At 40 wt% tackifier the shear resistance decreased, with the LTL (17k, 0.35) sample failing after 111 ± 15 hours and the LTL (35k, 0.31) sample failing at 11 ± 6 hours. We attribute the decrease in shear resistance to chain pullout of PTDL chain ends in the diblock and homopolymer side products being accelerated by the addition of tackifier increasing chain mobility. Migration of tackifier to the hard domains could also compromise shear resistance, but the constant T_g of the PLLA end blocks across formulations does not support this mechanism. Similarly, the lower volume fraction LTL based PSA formulations exhibited poor shear resistance with cohesive failure of the PSA rapidly

upon addition of the static load. We attribute this to the poor microphase separation and low elasticity of the samples, as shown in the SAXS data and demonstrated by the peel and loop tack tests (Table S6).

Conclusions

In this work we demonstrated that long aliphatic chain containing β-lactones are a promising material for PSA development. TDL was successfully prepared *via* epoxide carbonylation and polymerized in a single-pot synthesis to produce PLLA end-block-containing triblock polymers. High PLLA volume fraction LTL triblock polymers (f_{PLLA} = 0.31–0.35) were effective as the polymer component of PSA formulations employing a rosin ester tackifier. These materials showed excellent peel and loop tack performance consistent with commercial PSAs. The shear resistance of the formulations at lower tackifier loadings were good with a decrease in performance when 40 wt% tackifier was added. We attribute this to increased chain mobility in the midblock from the additional tackifier leading to failure by chain pullout. The PTDL midblocks displayed side-chain crystallinity with a melting temperature of −26 °C which was suppressed by the addition of tackifier allowing for a wide range of usage temperatures. Future work in this area should focus on increasing the molar mass of the poly(β-tridecalactone) midblock to achieve larger overall molar masses and more effective PLLA end blocks. Degradation studies of these materials should also be conducted to demonstrate their utility as biodegradable adhesives and alternative tackifiers explored, as the Sylvalite RE 80HP used here has shown limited hydrolytic degradability.[16] These materials have the potential to be commercially sourced from plant oils, and we have highlighted that they have commercially competitive properties which warrants further research.

Conflicts of interest

There are no conflicts to declare.

Data availability

The data will be published under a Creative Commons (CC0) license and stored in the Data Repository for the University of Minnesota (https://hdl.handle.net/11299/166578). Supplementary information (SI): materials, additional experimental details, additional data: ^{1}H and ^{13}C NMR analysis of products, SEC of polymers, DSC thermal characterization, SAXS and WAXS of films, rheological analysis, mechanical properties, peel and loop tack curves, images of failure modes. See DOI: https://doi.org/10.1039/d5lp00389j.

Acknowledgements

This work was supported by Bostik, an Arkema company. Research reported in this publication was supported by the Office of the Vice President of Research, College of Science and Engineering, and the Department of Chemistry at the University of Minnesota. We also acknowledge support from the National Science Foundation (CHE-2403983). We would like to thank Dr Mara Kuenen, Dr Daniel Krajovic, and Maggie Kumler for helpful discussions about the project along with Steven Gray, Dr. Darius Deak, and Dr. Nolan Mitchell of Bostik for their support. The SAXS and WAXS analysis was performed at the DuPont-Northwestern-Dow Collaborative Access Team (DND-CAT) located at Sector 5 of the Advanced Photon Source (APS). DND-CAT is supported by Northwestern University, The Dow Chemical Company, and DuPont de Nemours, Inc. This research used resources of the Advanced Photon Source, a U.S. Department of Energy (DOE) Office of Science User Facility operated for the DOE Office of Science by Argonne National Laboratory under Contract No. DE-AC02-06CH11357. Data was collected using an instrument funded by the National Science Foundation under Award Number 0960140. Research reported in this publication was supported by the Office of the Director, National Institutes of Health, under Award Number S10OD011952. The content is solely the responsibility of the authors and does not necessarily represent the official views of the National Institutes of Health.

References

1 C. Creton, Pressure-Sensitive Adhesives: An Introductory Course, *MRS Bull.*, 2003, **28**(6), 434–439.
2 D. M. Fitzgeral, Y. L. Colson and M. W. Grnstaff, Synthetic pressure sensitive adhesives for biomedical applications, *Prog. Polym. Sci.*, 2023, **142**, 101692.
3 J. H. Back, D. Baek, K. B. Sim, G. Y. Oh, S. W. Jang, H. J. Kim and Y. Kim, Optimization of Recovery and Relaxation of Acrylic Pressure-Sensitive Adhesives by Using UV Patterning for Flexible Displays, *Ind. Eng. Chem. Res.*, 2019, **58**(10), 4331–4340.
4 Y. Wang, C. Marcello, N. Sawant, A. Salam, S. Abubakr, D. Qi and K. Li, Identification and characterization of sticky contaminants in multiple recycled paper grades, *Cellulose*, 2023, **30**, 1957–1970.
5 P. Foster, T. Breton and E. Bird, Identifying the Source and Scale of Plastic in Compost Derived from Household and Commercial Food Waste. Report No. 463; Environmental Protection Agency of Ireland: 2024; https://www.epa.ie/publications/research/epa-research-2030-reports/research-463-identifying-the-source-and-scale-of-plastic-in-compost-derived-from-household-and-commercial-food-waste.php (accessed 2025-05-15).
6 N. Ballard, Designing acrylic latexes for pressure-sensitive adhesives: a review, *Polym. Int.*, 2024, **73**, 75–87.

7 E. Cohen, O. Binshtok, A. Dotan and H. Dodiuk, Prospective materials for biodegradable and/or biobased-pressure sensitive adhesives: a review, *J. Adhes. Sci. Technol.*, 2013, **27**(18–19), 1998–2013.
8 X. Wang, Y. Cao, J. Zhang and H. Yu, Biodegradable Polyurethane Pressure-Sensitive Adhesives Using Biobased Polyols with Distinct Intrinsic Properties, *ACS Appl. Polym. Mater.*, 2024, **6**, 5121–5128.
9 S. J. Hur, Y. Jeon, H. Jeong, J. Shim, J. Shin, K. Y. Choi, U. H. Choi and H. J. Kim, Biodegradable polyurethane non-tackifier pressure-sensitive adhesive derived from cashew nut shells, *Green Chem.*, 2026, DOI: 10.1039/D5GC05627F.
10 E. M. Brogden, P. F. Wilson, S. Hindmarsh, I. Hands-Portman, A. Unsworth, E. Liarou and S. A. F. Bon, A mesh reinforced pressure-sensitive adhesive for a linerless label design, *RSC Appl. Polym.*, 2024, **2**, 248–261.
11 C. Gao, K. C. Poon and C. K. Williams, Pressure-sensitive adhesives from polyester pentablock copolymers, *Polym. Chem.*, 2026, **17**, 21.
12 D. M. Krajoviv, M. S. Kumler and M. A. Hillmyer, PLA Block Polymers: Versatile Materials for a Sustainable Future, *Biomacromolecules*, 2025, **26**(5), 2761–2783.
13 J. Shin, M. T. Martello, M. Shrestha, J. E. Wissinger, W. B. Tolman and M. A. Hillmyer, Pressure-Sensitive Adhesives from Renewable Triblock Copolymers, *Macromolecules*, 2011, **44**, 87–94.
14 T. R. Ewert, A. M. Mannion, M. L. Coughlin, C. W. Macosko and F. S. Bates, Influence of rheology on renewable pressure-sensitive adhesives from a triblock copolymer, *J. Rheol.*, 2018, **62**(1), 161–170.
15 H. J. Kim, K. Jin, J. Shim, W. Dean, M. A. Hillmyer and C. J. Elison, Sustainable Triblock Copolymers as Tunable and Degradable Pressure Sensitive Adhesives, *ACS Sustainable Chem. Eng.*, 2020, **8**, 12036–12044.
16 S. Liang, D. M. Krajovic, B. D. Hoehn, C. J. Ellison and M. A. Hillmyer, Engineering Aliphatic Polyester Triblock Copolymer-Tackifier Blends for Hydrolytically Degradable Pressure Sensitive Adhesives, *ACS Appl. Polym. Mater.*, 2025, **7**, 1411–1420.
17 C. Xu, L. Wang, Y. Liu, H. Niu, Y. Shen and Z. Li, Rapid and Controlled Ring-Opening (Co)Polymerization of Bio-Sourced Alkyl-δ-Lactones To Produce Recyclable (Co) Polyesters and Their Application as Pressure-Sensitive Adhesives, *Macromolecules*, 2023, **56**, 6117–6125.
18 S. Lee, K. Lee, Y. W. Kim and J. Shin, Preparation and Characterization of a Renewable Pressure-Sensitive Adhesive System Derived from ε-Decalactone, L-Lactide, Epoxidized Soybean Oil, and Rosin Ester, *ACS Sustainable Chem. Eng.*, 2015, **3**, 2309–2320.
19 S. Chikkali and S. Mecking, Refining of plant oils to chemicals by olefin metathesis, *Angew. Chem., Int. Ed.*, 2012, **51**, 5802–5808.
20 Z. Zhou, K. Zhang, P. He, H. Chang, M. Zhang, T. Yan, X. Zhang, L. Yongwang and Z. Cao, Reactive Intermediate Confinement in Beta Zeolites for the Efficient Aerobic Epoxidation of α-Olefins, *Angew. Chem., Int. Ed.*, 2025, **64**, e202419900.
21 D. K. Schneiderman and M. A. Hillmyer, Aliphatic polyester block polymer design, *Macromolecules*, 2016, **49**, 2419–2428.
22 J. P. MacDonald, M. P. Parker, B. W. Greenland, D. Hermida-Merino, I. W. Hamley and M. P. Shaver, Tuning thermal properties and microphase separation in aliphatic polyester ABA copolymers, *Polym. Chem.*, 2015, **6**, 1445.
23 Y. D. Y. L. Getzler, V. Mahadevan, E. B. Lobkovsky and G. W. Coates, Synthesis of â-Lactones: A Highly Active and Selective Catalyst for Epoxide Carbonylation, *J. Am. Chem. Soc.*, 2002, **124**(7), 1174–1175.
24 A. K. Hubbell, J. R. Lamb, K. Klimovica, M. Mulzer, T. D. Shaffer, S. N. MacMillan and G. W. Coates, Catalyst-Controlled Regioselective Carbonylation of Isobutylene Oxide to Pivalolactone, *ACS Catal.*, 2020, **10**(21), 12537–12543.
25 J. Jiang, S. Rajendiran and S. Yoon, Double Ring-Expanding Carbonylation Using an In Situ Generated Aluminum Phthalocyanine Cobalt Carbonyl Complex, *Asian J. Org. Chem.*, 2019, **8**, 151–154.
26 T. L. Church, Y. D. Y. L. Getzler and G. W. Coates, The Mechanism of Epoxide Carbonylation by [Lewis Acid]$^+$[Co(CO)4]$^-$ Catalysts, *J. Am. Chem. Soc.*, 2006, **128**(31), 10125–10133.
27 A. Couffin, B. Martín-Vaca, D. Bourissou and C. Navarro, Selective O-acyl ring-opening of b-butyrolactone catalyzed by trifluoromethane sulfonic acid: application to the preparation of well-defined block copolymers, *Polym. Chem.*, 2014, **6**, 161.
28 L. Yang, Y. Y. Zhang, G. W. Yang, R. Xie and G. P. Wu, Controlled Ring-Opening Polymerization of β-Butyrolactone ViaBifunctional Organoboron Catalysts, *Macromolecules*, 2021, **54**, 5509–5517.
29 J. P. MacDonald and M. P. Shaver, *Aluminum Salen and SalanPolymerization Catalysts: From Monomer Scope to MacrostructureControl. In Green Polymer Chemistry: Biobased Materials andBiocatalysis*, American Chemical Society, 2015, pp. 147–167.
30 K. Teranishi, M. Iida, T. Araki, S. Yamashita and H. Tani, Stereospecific Polymerization of β-Alkyl- β-propiolactone, *Macromolecules*, 1974, **7**(4), 421–427.
31 C. Creton, A. Roos and A. Chiche, Effect of the Diblock Content on the Adhesive and Deformation Properties of PSAs Based on Styrenic Block Copolymers, in *Adhesion, Current Research and Applications*, Wiley-VCH, Weinheim, 2005, pp. 337–364.
32 S. Liang, C. J. Ellison and M. A. Hillmyer, Tunable adhesion properties of hydrolytically degradable aliphatic polyester triblock/diblock copolymer blends, *Polym. Chem.*, 2025, **16**, 3511–3522.
33 K. C. Daoulas, D. N. Theodorou, A. Roos and C. Creton, Experimental and Self-Consistent-Field Theoretical Study

of Styrene Block Copolymer Self-Adhesive Materials, *Macromolecules*, 2004, **37**(13), 5093–5109.

34 G. Kim and M. Libera, Morphological Development in Solvent-Cast Polystyrene-Polybutadiene-Polystyrene (SBS) Triblock Copolymer Thin Films, *Macromolecules*, 1998, **31**, 2569–2577.

35 H. Yokoyama, Diffusion of block copolymers, *Mater. Sci. Eng., R*, 2006, **53**, 199–248.

36 A. Watts, N. Kurokawa and M. A. Hillmyer, Strong, Resilient, and Sustainable Aliphatic Polyester Thermoplastic Elastomers, *Biomacromolecules*, 2017, **18**(6), 1845–1854.

37 D. M. Krajovic, G. Haugstad and M. A. Hillmyer, Crystallinity-Independent Toughness in Renewable Poly(L-lactide) Triblock Plastics, *Macromolecules*, 2024, **57**, 2818–2834.

38 S. Liffland and M. A. Hillmyer, Enhanced Mechanical Properties of Aliphatic Polyester Thermoplastic Elastomers through Star Block Architectures, *Macromolecules*, 2021, **54**(20), 9327–9340.

39 K. A. O'Leary and D. R. Paul, Physical properties of poly(n-alkyl acrylate) copolymers. Part 1. Crystalline/crystalline combinations, *Polymer*, 2006, **47**, 1226–1244.

40 E. P. Chang, Viscoelastic Windows of Pressure-Sensitive Adhesives, *J. Adhes.*, 1991, **34**(1–4), 189–200.

41 A. J. Peters and T. P. Lodge, Comparison of Gel Relaxation Times and End-Block Pullout Times in ABA Triblock Copolymer Networks, *Macromolecules*, 2016, **49**, 7340–7349.